ELSEVIER

Journal of Power Sources 80 (1999) 39–45

JOURNAL OF POWER SOURCES

Electrochemical characteristics of the interface between the metal hydride electrode and electrolyte for an advanced nickel/metal hydride battery

Jianwen Han [a], Feng Feng [a], Mingming Geng [a], Robert Buxbaum [b], Derek O. Northwood [c,*]

[a] *Mechanical and Materials Engineering, University of Windsor, Windsor, Ontario, Canada N9B 3P4*
[b] *Chemical Engineering Department, Michigan State University, East Lansing, MI 48824, USA*
[c] *Faculty of Engineering and Applied Science, Ryerson Polytechnic University, 350 Victoria Street, Toronto, Ontario, Canada M5B 2K3*

Abstract

The characteristics of the negative electrode of a Ni/MH (metal hydride) battery are related to the charge transfer and mass transfer processes at the interface between the MH electrode and the electrolyte. With increasing number of charge/discharge cycles, the MH alloy powders micro-crack into particles that are several microns in diameter and this then influences the exchange current density. A polarization experiment was used to analyze the charge transfer and mass transfer processes. The exchange current densities of uncoated and Pd-coated $Mm_{0.95}Ti_{0.05}Ni_{3.85}Co_{0.45}Mn_{0.35}Al_{0.35}$ alloy electrodes increase with increasing number of charge/discharge cycles before reaching a constant value after 20–30 cycles.

Keywords: Metal hydrides; Nickel/metal hydride batteries; Electrode reactions

1. Introduction

The need for high energy density storage batteries has been growing in recent years. The advent of electric vehicles (EVs), portable computers, cellular telephones, and new cordless appliances and tools has made this need even more urgent. Although conventional storage batteries such as nickel–cadmium (Ni/Cd) and lead–acid batteries have been further improved in design and packaging in the past several years, there is still a need for improved performance and power density. The innate toxicity of cadmium and lead has also come under scrutiny. The development of EVs aims to develop an advanced battery pack with high energy density, high specific power and long cycle lifetime. In the EV battery pack, it is also necessary to develop a battery management system to monitor the over-charge and over-discharge of each battery module, especially for the lead–acid, Ni/Cd and lithium-ion batteries.

The use of metal hydrides as active negative electrode materials in rechargeable alkaline batteries has been studied for a long time. Although Ni/MH batteries have superior specific energy than the other two major aqueous electrolyte systems (lead–acid and Ni/Cd), they remain largely inferior to the new rechargeable lithium (Li-ion) batteries. However, lithium batteries are much more expensive to produce. It has been estimated [1] that the approximate cost (per Wh) for Ni/Cd, Ni/MH and Li-ion batteries are in the ratios of 1:1.35:2–3, respectively.

In addition, lithium batteries cannot be operated for a safety reasons without electronic control of each individual cell, because the lithium batteries are very sensitive to over-charge and over-discharge. The over-charge and over-discharge performance of the Ni/MH battery are better than other batteries.

According to Belkbir et al.'s results [2], the particle size of a $LaNi_5$-based alloy powder decreases greatly in the first five cycles and then remains constant at micron-sized particles with an increasing number of cycles. The alloy powders are easily oxidized in the early hydrogen absorption/desorption cycles during which the particles are broken-up with each cycle and then resist further oxidation after the particle size reaches a constant value and there is no further attrition.

The electrochemical reactions take place at the interface between the MH alloy powder and electrolyte. and are composed of charge-transfer process and mass-transfer processes. Yang et al. [3] considered hydrogen transfer

* Corresponding author. E-mail: dnorthwo@acs.ryerson.ca

0378-7753/99/$ - see front matter
PII: S0378-7753(98)00250-X

through the interface and established a general relationship between the overpotential and the rate of hydrogen diffusion in the electrodes as well as the kinetic parameters characterizing the transfer from the absorbed to the adsorbed state. Zheng et al. [4] established a porous electrode theory to estimate the exchange current density, the polarization resistance and the transfer coefficient for an $LaNi_{4.27}Sn_{0.24}$ hydride electrode in an alkaline solution. The conventional Tafel polarization method cannot be applied for the porous metal hydride system due to the presence of the internal mass transfer effects and the internal ohmic voltage drop of the electrode.

The MH alloy powders in the negative electrode of an Ni/MH battery will break up into the micron-sized particles with increasing the number of charge/discharge cycles. At the same time, the smaller particles are easily oxidized and lose their hydrogen absorption capacity. X-ray photoelectron spectroscopy (XPS) studies have shown that the oxygen concentration in the surface of grains of an AB_5-type alloy reaches about 10 at.% after 270 cycles (40% DOD) and about 30 at.% after 1080 cycles (40% DOD) at a depth of 100 nm [1]. Meli et al. [5] have also studied the oxidation of $LaNi_5$-based alloy powders during charge/discharge cycles by means of the XPS technique and have found that after 30 charge/discharge cycles, the $La/LaNi_5$ ratio was about two and the $(Ni + Co)/LaNi_5$ ratio was about four at depths of 2–40 nm.

In this study, uncoated and Pd-coated $Mm_{0.95}Ti_{0.05}Ni_{3.85}Co_{0.45}Mn_{0.35}Al_{0.35}$ alloy powders were used as the negative electrode material of an experimental cell and the specific capacity, exchange current density and electrochemical stability was determined.

2. Experimental details

A hydrogen storage alloy of nominal composition $Mm_{0.95}Ti_{0.05}Ni_{3.85}Co_{0.45}Mn_{0.35}Al_{0.35}$ (where Mm denotes Mischmetal, comprising 43.1 wt.% La, 3.5 wt.% Ce, 13.3 wt.% Pr and 38.9 wt.% Nd) was prepared by induction melting and rapid cooling. The alloy ingot was mechanically pulverized to obtain a sifted particle size around 45–53 μm. Some of the alloy powder was coated electrolessly with palladium using the method of Buxbaum and Hsu [6]. Both uncoated and Pd-coated alloys were used as the negative electrode material in the experimental cells. The positive electrode in these cells, a sintered $Ni(OH)_2/NiOOH$ plate, was obtained from a commercial supplier.

The set-up of the experimental cells was in a sintered glass apparatus with three compartments. The negative electrode was placed in the central compartment and two $Ni(OH)_2/NiOOH$ electrodes were placed on either side. For the specific capacity and exchange current density measurements, the MH alloy powders were mixed with nickel powder in a weight ratio of 1:1 together with a small amount (3 wt.%) of polytetrafluoroethylene (PTFE) aqueous solution as a binder and then pressed in a cylindrical press at a pressure of 500 MPa. A pellet with a diameter of 10 mm and thickness of 0.8 mm was formed at room temperature. The emphasis of these charge/discharge tests was on the electrochemical stability of the negative electrode. Thus the capacity of the positive electrode plates was designed to be higher than that of the negative electrode. Two negative electrode plates for different experimental cells were made from uncoated and Pd-coated $Mm_{0.95}Ti_{0.05}Ni_{3.85}Co_{0.45}Mn_{0.35}Al_{0.35}$ alloy powder, respectively. To make the negative electrode plates for two experimental cells, 0.1 g of each alloy powder was separately used. The electrolyte in the cells was a 6 M KOH aqueous solution.

The charge/discharge and polarization tests of the experimental cells were conducted using a Solartron 1285 potentiostat with CorrWare software for Windows. The testing resolution of the potential, current and time is 0.1 mV, 0.1 mA and 0.1 s, respectively. The charge and discharge regimes were conducted in an air-conditioned room at a temperature of 23 ± 1°C. The experimental cells were cycled over 40 times. They were charged at a current of 120 mA g^{-1} for 3 h and discharged at a current of 120 mA g^{-1} to an end-of-discharge-potential of -0.5 V. The measurements of the polarization curves were obtained under potentiodynamic conditions at a scan rate of 1 mV s^{-1}. The polarization curve was tested after fully charging and the open-circuit potential was stabilized (the variation in the potential was less than 1 mV for 1 h). Based on a set-up of the Solartron 1285 potentiostat, the anodic polarization current and overpotential are defined as positive values.

3. Results and discussion

3.1. Specific capacity

The hydrogen-absorbing alloy, $Mm_{0.95}Ti_{0.05}Ni_{3.85}Co_{0.45}Mn_{0.35}Al_{0.35}$, that was developed for the negative electrode, was based on the $MmNi_5$-based alloy with partial replacement of Ni by Co, Mn and Al elements and Mm by Ti. It should be noted that the addition of Mn was used to increase the crystal cell volume, and to achieve an increase in specific capacity and better high-rate dischargeability. The addition of Ti was used to adjust the stoichiometric composition of the AB_5 alloy in order to give an increase in the anti-pulverization capability. In the KOH aqueous solution, the standard redox potentials of the rare earth elements, also Al, Mn and Ti range from -1.37 V to -1.05 V vs. SHE. These metallic elements are easily oxidized to form a stable metal oxide compounds at the surface of the alloy powder. These oxides, as passivation

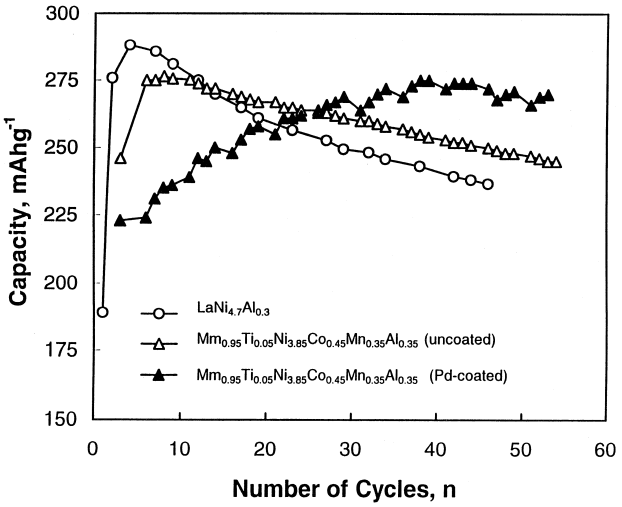

Fig. 1. Variation of the discharge capacity of uncoated and Pd-coated $Mm_{0.95}Ti_{0.05}Ni_{3.85}Co_{0.45}Mn_{0.35}Al_{0.35}$ alloy electrodes with number of charge/discharge cycles at 25°C.

phases, are used both to prevent further oxidation of the MH alloy powder and to increase the charge/discharge cycle lifetime.

Fig. 1 shows the discharge capacity of the uncoated and Pd-coated $Mm_{0.95}Ti_{0.05}Ni_{3.85}Co_{0.45}Mn_{0.35}Al_{0.35}$ alloy electrodes as a function of number of cycles. The discharge capacity of the cell made by using uncoated $Mm_{0.95}Ti_{0.05}Ni_{3.85}Co_{0.45}Mn_{0.35}Al_{0.35}$ alloy powder as negative electrode reaches 276 mA h g^{-1} after 5 cycles and decreases slowly on cycling, and finally decreases to about 250 mA h g^{-1} after 40 cycles. The discharge capacity of a cell made from Pd-coated $Mm_{0.95}Ti_{0.05}Ni_{3.85}Co_{0.45}Mn_{0.35}Al_{0.35}$ alloy increases continuously from a specific capacity of 225 mA h g^{-1} at the beginning of cycle to a maximum value of 275 mA h g^{-1} after 40 cycles and then the capacity slowly decreases. The decay in capacity results from a deterioration of the negative electrode made from the MH alloy powder. The deterioration is due to oxidation and pulverization of the MH alloy powder with increasing charge/discharge cycles. It can be seen from Fig. 1 that discharge capacity of the alloy powders shows a large variation for the first 30 cycles and this variation is due to the deterioration of the negative electrode. It is believed that many of the grain boundaries in the MH alloy ingot have layers of segregated rare earth elements such as La that are susceptible to corrosion [7]. These layers are corroded in the alkaline electrolyte and are deposited on the surface of grain particles as needle-shaped $La(OH)_3$. This results in an increase of electrode resistance, which in turn decreases the alloy capacity.

3.2. Linear polarization

In an alkaline aqueous solution, the hydrogen atoms produced at the surface of the MH alloy powder are instantly adsorbed and then diffuse into the bulk of the MH alloy. The electrochemical reactions can therefore be expressed as follows:

$$H_2O + e^- \Leftrightarrow H_{ad} + OH^- \quad (1)$$

and

$$H_{ad} \Leftrightarrow H_{ab} \quad (2)$$

where H_{ad} and H_{ab} denote the hydrogen atoms on the surface of the MH alloy powder and in the bulk of MH alloy, respectively.

Reaction (1) reflects the charge transfer process at the interface between the MH alloy powder and the electrolyte, and reaction (2) relates to the diffusion of hydrogen from the powder surface to the bulk of the MH alloy.

The electrochemical kinetics of the charge transfer process were determined by dc polarization methods. The slope of the linear polarization curve represents the electrode resistance (R_e). The electrode resistance is composed of the ohmic resistance (R_Ω) and the polarization resistance (R_p). The polarization resistance is mainly determined by the charge transfer process at the interface between the MH electrode and the electrolyte. The charge transfer process can be described by using the exchange current density. The exchange current density can be calculated from the polarization resistance in the charge transfer process, as follows:

$$R_p = \frac{RT}{Fi_0} \quad (3)$$

where R is the gas constant, T the temperature, F the Faraday constant and i_0 the exchange current density. Since the magnitude of R_Ω is very small compared to R_p, the slope of the linear polarization curve can generally be used to estimate the exchange current density.

The polarization curves for both uncoated and Pd-coated $Mm_{0.95}Ti_{0.05}Ni_{3.85}Co_{0.45}Mn_{0.35}Al_{0.35}$ alloy electrodes are shown in Fig. 2a and b, respectively. The value of the exchange current density was calculated from the slope of the linear polarization curves of potential vs. current. The linear polarization curves were measured at a small polarization current, comparing to the exchange current density, i_0, or at a small polarization overpotential (< 30 mV).

The exchange current densities vs. the number of charge/discharge cycles for both alloy electrodes are shown in Fig. 3. An increase in the exchange current density with number of cycles reflects the fast hydrogen adsorption process at the interface between the MH alloy powder and the electrolyte. The exchange current density of the uncoated $MmNi_5$-based alloy electrode reaches 164 mA g^{-1} after 20 cycles and then it slowly increases to a value of about 230 mA g^{-1} after 50 cycles. Similarly, the exchange current density of the Pd-coated $MmNi_5$-based alloy electrode reaches 172 mA g^{-1} after 20 cycles and then increases to a value of about 267 mA g^{-1} after 50 cycles. In comparison, the discharge capacity of the uncoated $Mm_{0.95}Ti_{0.05}Ni_{3.85}Co_{0.45}$ $Mn_{0.35}$ $Al_{0.35}$ alloy pow-

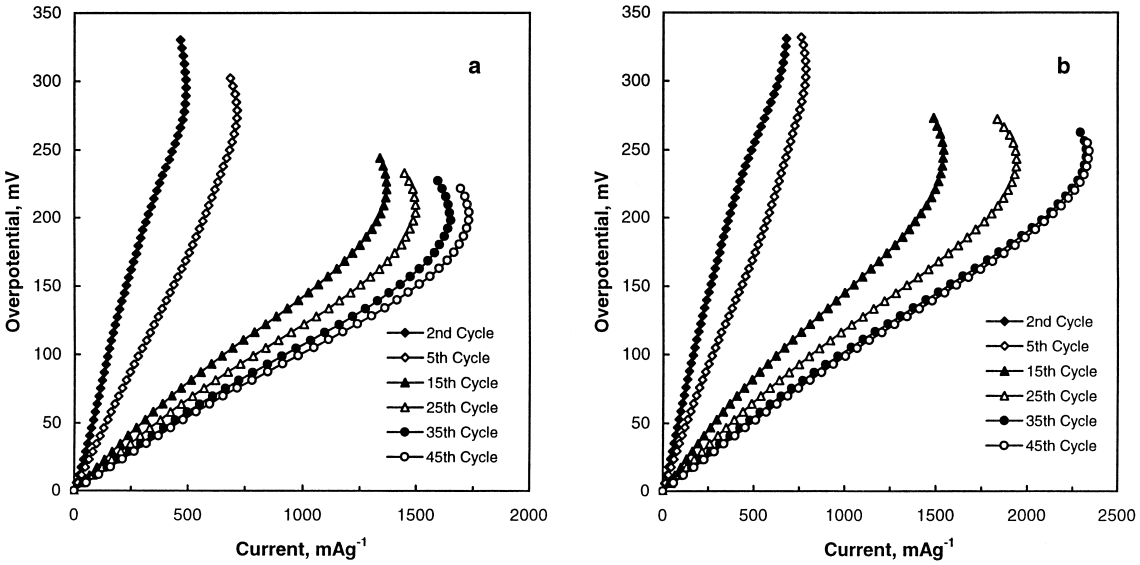

Fig. 2. Polarization curves of η vs. i for: (a) uncoated and (b) Pd-coated $Mm_{0.95}Ti_{0.05}Ni_{3.85}Co_{0.45}Mn_{0.35}Al_{0.35}$ alloy electrodes determined at a scan rate of 1 mV s^{-1}.

der decreases after 10 cycles, because of the oxidation and pulverization of the alloy powder. The value of the polarization resistance is inversely proportional to that of the exchange current density. In other words, the capacity decay of the alloy powders will not result in an increase of the polarization resistance. Since the exchange current densities of both uncoated and Pd-coated MmN_5-based alloy electrodes remain almost constant after 30 cycles, this implies that the charge transfer process at the interface between the MH alloy powder and electrolyte is stabilized, i.e., the electrochemical reaction for hydrogen adsorption at the interface is stabilized.

3.3. Effects of mass transfer on the polarization

When the polarization current is larger than the exchange current density, the electrochemical reactions are controlled by charge transfer and mass transfer processes. The electrode potential of the MH alloy electrode is far removed from the equilibrium potential, typically at an overpotential, η, of about 100 mV. The overpotential of the MH electrode, η, is composed of the charge transfer overpotential, η_t, and mass transfer overpotential, η_m. The charge transfer overpotential is proportional to $\ln(i)$ and the mass-transfer overpotential is proportional to the logarithm of the reactant concentration. For anodic polarization, polarization leads to a decrease in activation energy of the oxidation reaction. An increase in the oxidation reaction rate, meanwhile, leads to an increase in the activation energy of reduction reaction and a decrease in a rate of the reduction reaction. Therefore the reduction reaction in the anodic polarization process can be neglected in comparison with the rate of oxidation reaction.

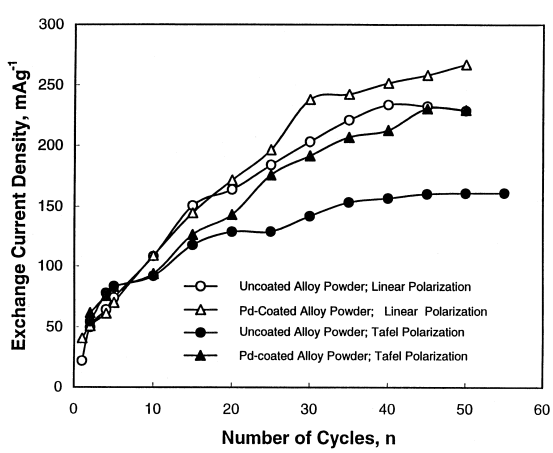

Fig. 3. Exchange current densities of uncoated and Pd-coated $Mm_{0.95}Ti_{0.05}Ni_{3.85}Co_{0.45}Mn_{0.35}Al_{0.35}$ alloy electrodes as a function of number of charge/discharge cycles.

Based on the concept of free energy curves and Fick's law, the anodic overpotential can be expressed as follows [8,9]:

$$\eta = \frac{RT}{(1-\alpha)F}\ln\left(\frac{i_L}{i_0}\right) + \frac{RT}{(1-\alpha)F}\ln\left(\frac{i}{i_L - i}\right) \qquad (4)$$

where η is the overpotential, α is the transfer coefficient, i_L is the limiting current.

From Eq. (4), a plot of η vs. $\ln(i/i_L - i)$ should produce a straight line in the middle range of the polarization curve with its slope being $RT/(1-\alpha)F$ and intercept $RT/(1-\alpha)F \ \ln(i_L/i_0)$. Therefore, α and i_0 can be calculated from data for i_L and T.

The overpotential of the uncoated and Pd-coated $Mm_{0.95}Ti_{0.05}Ni_{3.85}Co_{0.45}Mn_{0.35}Al_{0.35}$ alloy electrodes as a function of $\ln(i/(i_L - i)$ are shown in Fig. 4a and b. The calculated exchange current densities are shown in Fig. 3. Fig. 3 also shows that the exchange current densities evaluated from the polarization which includes effects of

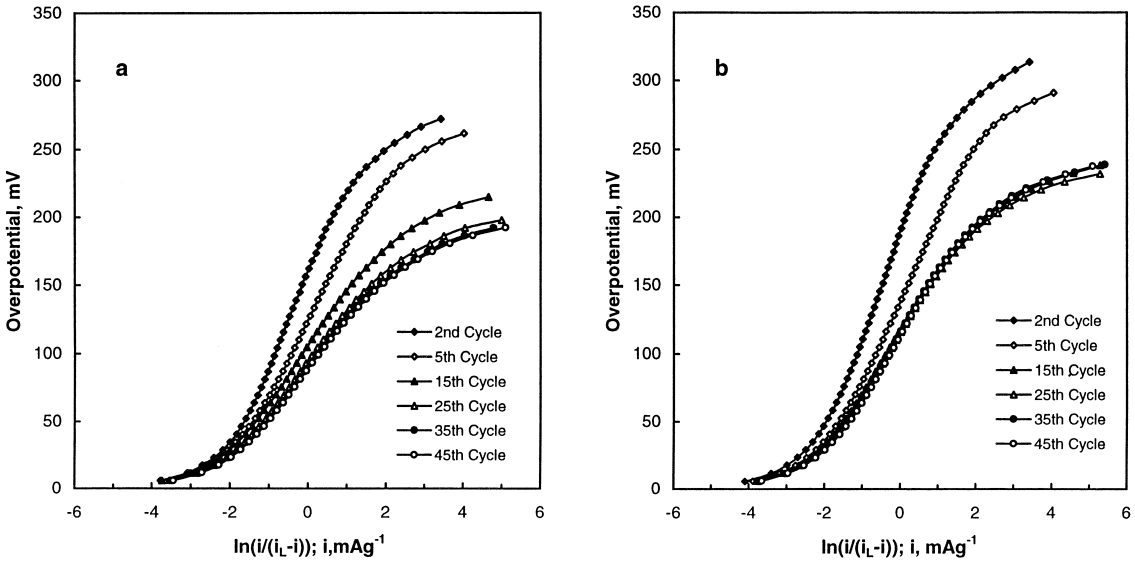

Fig. 4. The overpotential, η, of: (a) uncoated and (b) Pd-coated $Mm_{0.95}Ti_{0.05}Ni_{3.85}Co_{0.45}Mn_{0.35}Al_{0.35}$ alloy electrodes as a function of $\ln(i/(i_L - i))$.

the mass transfer process are lower than those calculated from linear polarization. For more than 20 charge/discharge cycles, there is a larger difference between i_0 for linear polarization and that for polarization which includes the effects of mass transfer. Generally, the ohmic polarization increases with increasing polarization potential. The ohmic polarization at higher overpotential leads to a decrease in the polarization current and also leads to a decrease in the limiting current. Thus the exchange current densities, obtained by the polarization curves which include the effects of mass transfer process in both alloy electrodes, are influenced by the ohmic polarization, which results in a decrease in the limiting current. The reason of the difference in the exchange current densities between the uncoated and Pd-coated MH alloy electrodes may result from a larger exchange current density for hydrogen absorption at the surface of Pd layer. The exchange current density of hydrogen at the interface between Pd and the electrolyte is much larger than that at the interface between MH alloy powder and the electrolyte.

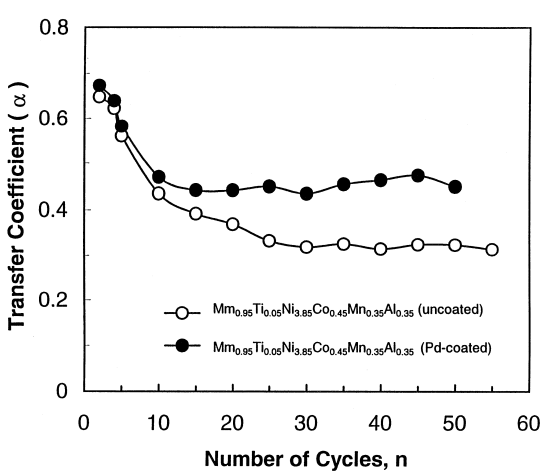

Fig. 5. Transfer coefficient of uncoated and Pd-coated $Mm_{0.95}Ti_{0.05}Ni_{3.85}Co_{0.45}Mn_{0.35}Al_{0.35}$ alloy electrodes as a function of number of cycles.

The transfer coefficient, α, was also evaluated from the relationship between overpotential, η, and $\ln(i/(i_L - i))$, and is shown in Fig. 5. The transfer coefficient decreases with increasing the number of cycles for both uncoated and Pd-coated MH alloy electrodes. The transfer coefficient for uncoated MH alloy electrode decreases from 0.65 after one cycle to 0.33 after 25 cycles and then remains constant at a value of 0.32. The transfer coefficient for the Pd-coated MH alloy electrode decreases from 0.67 after one cycle to 0.44 after 15 cycles and then remains constant.

Thus the Pd-coated MH alloy electrode more readily reaches stable performance upon cycling than the uncoated MH alloy electrode.

With an increasing number of charge/discharge cycles, the MH alloy powders will micro-crack and be pulverized into micron-sized particles, because of the expansion of crystal cells through hydrogen absorption and desorption. This micro-cracking leads to an increase in the reaction surface area and an improvement in activation for H adsorption at the electrode/electrolyte interface. and so increases the hydrogen exchange current densities. Both the uncoated and Pd-coated $MmNi_5$-based alloy powders were pulverized and the decrease in the particle size leads to an increase in reaction surface area and exchange current density with increasing the number of cycles.

3.4. Variation of equilibrium potential with number of cycles

The polarization measurements of the electrodes were conducted after fully charging and after the open-circuit

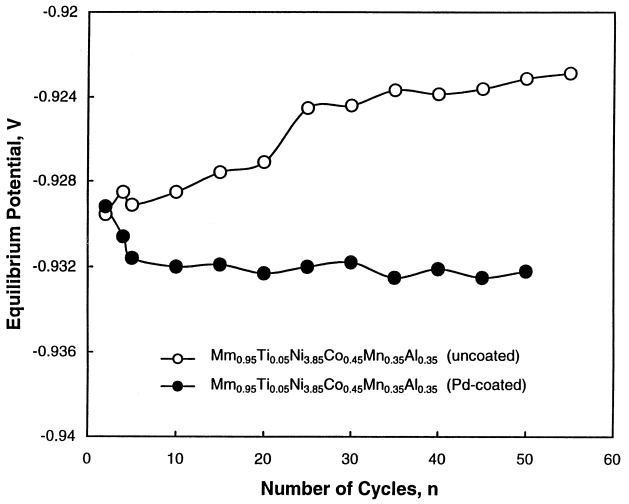

Fig. 6. Equilibrium potential of: (a) uncoated and (b) Pd-coated $Mm_{0.95}Ti_{0.05}Ni_{3.85}Co_{0.45}Mn_{0.35}Al_{0.35}$ alloy electrodes as a function of number of cycles.

potential had stabilized (i.e., a variation in the potential less than 1 mV for 1 h). At this time, the potential of the MH electrode approximately reaches an equilibrium state. The equilibrium potential of the electrodes as a function of number of charge/discharge cycles is shown in Fig. 6. It can be seen that the equilibrium potential of the uncoated $MmNi_5$-based alloy electrode increases by 7 mV after 20 cycles and then remains constant with increasing number of cycles. However, the equilibrium potential of the Pd-coated $MmNi_5$-based alloy electrode decreases by 4 mV after 5 cycles and then remains constant. The Pd layer at the surface of the MH alloy powder leads to a fast stabilization of the equilibrium potential of the MH electrode with cycles.

With increasing number of charge/discharge cycles, the MH alloy powder is pulverized into a micro-sized particles and the micro-sized particles show a distortion in the crystal structure and a fresh surface, which make hydrogen dissociation easier and result in a decrease in the hydrogen equilibrium pressure. Lundin and Lynch [10] believed that the hydrogen atoms occluded in the interstitial sites in the metal lattice and the resulting strain imposed on the lattice increased the interstitial hole size. The increase in the equilibrium potential of the uncoated alloy electrode is attributed to the larger interstitial hole size in the lattice which, in turn, leads to a decrease in the free energy. The decrease in the equilibrium potential of Pd-coated MH electrode is related to the fact that Pd-coating alloy electrode leads to an increase in the free energy of formation of the metal hydride, ΔG, and also to a positive increase in formation enthalpy, ΔH, of metal hydride (this from the thermodynamic relationship: $\Delta G = \Delta H - T\Delta S$, where the entropy, ΔS, changes only by a small amount for the metal hydride and ΔH can be considered as the main factor for evaluating the stability of metal hydride [11]). The formation enthalpy of metal hydride is defined as negative because it is an exothermic process, and the more negative the formation enthalpy, the more stable the metal hydride, and the more resistant it is to anodic oxidation. With increasing number of charge/discharge cycles, the Pd-coating at the surface of the MH alloy powder makes the formation enthalpy of the metal hydride more positive (smaller in absolute value), hence it decreases the resistance to anodic oxidation, and hence increases the reaction rate for anodic oxidation and the exchange current density.

The equilibrium potential can be expressed as follows:

$$E_{eq} = \left[E^0(H) - E^0(\mathrm{HgO/Hg})\right] + \frac{RT}{2F}\ln\left[\frac{a(\mathrm{H_2O})}{f(\mathrm{H_2})P(\mathrm{H_2})}\right] \quad (5)$$

where, $E^0(H) - E^0(\mathrm{HgO/Hg})$ is a difference in the potentials between the standard hydrogen electrode and HgO/Hg electrode. $f(\mathrm{H_2})$ is the hydrogen fugacity which is about 1.00059 at a temperature in a range of 273-− 298 K. $a(\mathrm{H_2O})$ is the water activity and it varies with the KOH concentration and temperature. A variation of the equilibrium potential, which results from a variation of $a(\mathrm{H_2O})$ with KOH concentration at a temperature of 298 K, is about 1 mV for an increase in 1 M KOH. $P(\mathrm{H_2})$ is the equilibrium pressure of hydrogen, and it is dependent on the hydrogen concentration in the MH alloy and the crystal structure of the MH alloy particles.

A variation of the equilibrium pressure of hydrogen, $(\ln[P(\mathrm{H_2})]$, is about -0.54 at the fully charged state for the uncoated alloy electrode during the first 20 cycles. Even though the equilibrium potential changes with temperature, it only increases about 0.3 mV for a temperature increase of 1 K. In this experiment, there was an increase of 7 mV in the equilibrium potential with cycling at the fully charged state, resulting mainly from a decrease in free energy or the hydrogen equilibrium pressure.

4. Conclusions

The main conclusions to come from this study are as follows.

The saturated discharge capacity of an uncoated $Mm_{0.95}Ti_{0.05}Ni_{3.85}Co_{0.45}Mn_{0.35}Al_{0.35}$ alloy electrode was 276 mA h g^{-1} and this decreased to 250 mA h g^{-1} after 40 charge/discharge cycles. The discharge capacity of a Pd-coated $MmNi_5$-based alloy electrode was 225 mA g^{-1} before cycling, and it increased to a maximum value of 275 mA h g^{-1} after 40 cycles, and then remained almost constant with increasing number of cycles.

Polarization measurements show that the exchange current densities of both alloy electrodes increase with increasing number of charge/discharge cycles.

The transfer coefficient decreases with increasing number of cycles for both alloys.

The Pd-coated alloy more readily reaches stable performance on cycling compared to the uncoated alloy.

The capacity decay of the alloy powders, which results from oxidation and pulverization, will not lead to an increase in the polarization resistance.

Micro-cracking activation, resulting from an increase in reaction surface area and an improvement in the electrode surface activation, increases the hydrogen exchange current densities.

Acknowledgements

Funding for this work is being provided by the Natural Science and Engineering Research Council of Canada through a Research Grant (A4391) awarded to Prof. Derek O. Northwood.

References

[1] P. Ruetschi, F. Meli, J. Desilvestro, J. Power Sources 57 (1995) 85.
[2] L. Belkbir, N. Gerard, A. Percheron-Guegan, J.C. Achard, Int. J. Hydrogen Energy 4 (1979) 541.
[3] Q.M. Yang, M. Ciureanu, D.H. Ryan, J.O. Strom-Olsen, J. Electrochem. Soc. 141 (1994) 2108.
[4] G. Zheng, B.N. Popov, R.E. White, J. Electrochem. Soc. 143 (1996) 435.
[5] F. Meli, T. Sakai, A. Zuttel, L. Schlapbach, J. Alloys Comp. 221 (1995) 284.
[6] R.E. Buxbaum, P.C. Hsu, U.S. Patent 5149420, 1992.
[7] J.J.G. Willems, Philips J. Res. 39 (1984) 1, Suppl. No. 1.
[8] A.J. Bard, L.R. Faulkner, Electrochemical Methods—Fundamentals and Applications, Wiley, New York, 1980, p. 109.
[9] H.W. Yang, Y.Y. Wang, C.C. Wan, J. Electrochem. Soc. 143 (1996) 432.
[10] C.E. Lundin, F.E. Lynch, Hydride for Energy Storage, Pergamon, Oxford, 1978, p. 385.
[11] Z.X. Zhou, C.H. He, Z.P. Wang, C.M. Wang, Acta Physico-Chimica Sinica 8 (1992) 558, (In Chinese).